Kim et al. Earth, Planets and Space (2016) 68:64
DOI 10.1186/s40623-016-0438-9

Earth, Planets and Space

FULL PAPER Open Access

The Nankai Trough earthquake tsunamis in Korea: numerical studies of the 1707 Hoei earthquake and physics-based scenarios

SatByul Kim[1], Tatsuhiko Saito[2], Eiichi Fukuyama[2] and Tae-Seob Kang[1*]

Abstract

Historical documents in Korea and China report abnormal waves in the sea and rivers close to the date of the 1707 Hoei earthquake, which occurred in the Nankai Trough, off southwestern Japan. This indicates that the tsunami caused by the Hoei earthquake might have reached Korea and China, which suggests a potential hazard in Korea from large earthquakes in the Nankai Trough. We conducted tsunami simulations to study the details of tsunamis in Korea caused by large earthquakes. Our results showed that the Hoei earthquake (Mw 8.8) tsunami reached the Korean Peninsula about 200 min after the earthquake occurred. The maximum tsunami height was ~0.5 m along the Korean coast. The model of the Hoei earthquake predicted a long-lasting tsunami whose highest peak arrived 600 min later after the first arrival near the coastline of Jeju Island. In addition, we conducted tsunami simulations using physics-based scenarios of anticipated earthquakes in the Nankai subduction zone. The maximum tsunami height in the scenarios (Mw 8.5–8.6) was ~0.4 m along the Korean coast. As a simple evaluation of larger possible tsunamis, we increased the amount of stress released by the earthquake by a factor of two and three, resulting in scenarios for Mw 8.8 and 8.9 earthquakes, respectively. The tsunami height increased by 0.1–0.4 m compared to that estimated by the Hoei earthquake.

Keywords: The 1707 Hoei earthquake, Tsunamis in Korea, Nankai earthquake tsunamis

Background

There have been five observed tsunami events on the Korean Peninsula since the 1900s, when instrumental records (e.g., tidal gauge) began. All tsunamis were caused by earthquakes occurring in Japan (Fig. 1). The first tsunami was observed on August 2, 1940, and was generated by the 1940 Shakotan-oki earthquake (Mw 7.5; Satake 1986). The earthquake did not result in any fatalities in Korea but did destroy houses and fishing vessels. The second tsunami was caused by the 1964 Niigata earthquake (Mw 7.5; Satake and Abe 1983), and there was no damage. The most destructive tsunami was generated by the 1983 Akita-oki earthquake (Mw 7.7; Fukuyama and Irikura 1986). One person was killed and two people went missing in Korea due to this tsunami. The maximum run-up height of ~4 m was recorded in Imwon Harbor, which is located on the eastern coastline of the Korean Peninsula. Another tsunami was caused by the 1993 southwest-off Hokkaido earthquake (Mw 7.8; Tanioka et al. 1995). The hypocenter of this earthquake was further from Korea than that of the 1983 Akita-oki earthquake, whereas the magnitude of both events was similar. As a result, the tsunami caused by the Hokkaido earthquake had less impact than that resulting from the 1983 Akita-oki earthquake, but also caused damage to vessels.

Although the previous disastrous earthquakes to Korea occurred in the backarc region, these earthquakes were all less than M8 earthquakes. However, in the forearc region there is a possibility that large M9 earthquakes may occur (Parsons et al. 2012). The most recent tsunami observed at Jeju Island is from the 2011 Tohoku-oki earthquake, which was generated in the forearc region, and tsunami heights of ~0.2 m were recorded by tidal

*Correspondence: tskang@pknu.ac.kr
[1] Department of Earth and Environmental Sciences, Pukyong National University, 45 Yongso-ro, Nam-gu, Busan 48513, Republic of Korea
Full list of author information is available at the end of the article

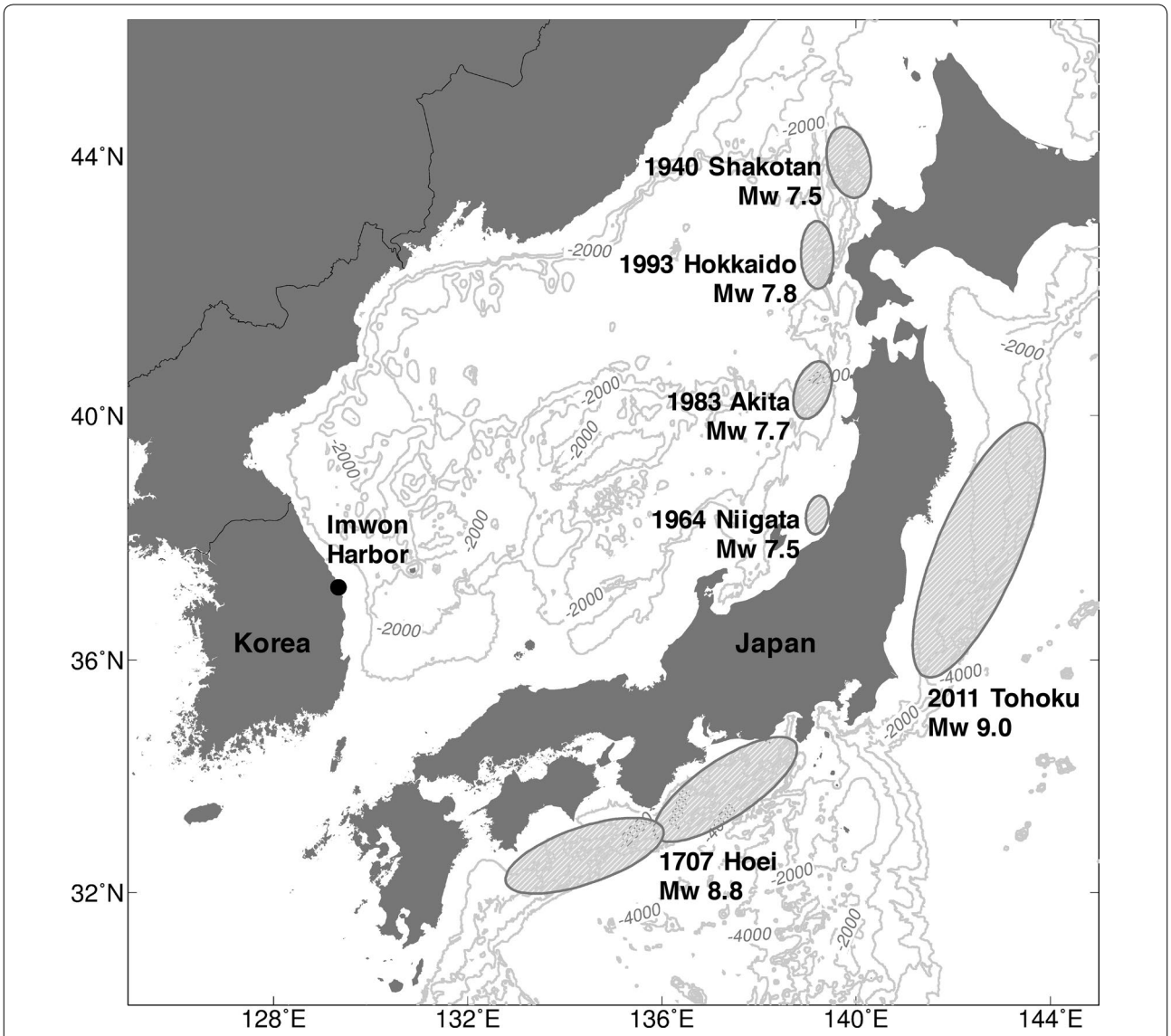

Fig. 1 Distribution of tsunami sources around Korea and Japan. *Gray ellipses* indicate tsunami sources caused by earthquakes. Bathymetry contours are plotted at intervals of 2000 m

gauges along the coast of the island. There are no instrumental records showing that Korea was affected by tsunamis from the Nankai Trough, located off the coast of southwest Japan, where large earthquakes repeatedly occur at intervals of about 100–200 years (e.g., Kumagai 1996; Ishibashi and Satake 1998). This raises an interesting question: If a large earthquake occurs in an area along the Nankai Trough, which is closer to the Korean Peninsula, what would be the size of the resulting tsunami?

The Nankai Trough area is a long subduction zone where the Philippine Sea Plate subducts beneath the Eurasian Plate, and extends approximately 600–800 km from the Izu Peninsula to the southeast side of Kyushu Island (Fig. 2). The Nankai Trough region is usually divided into four or five segments, and the earthquakes are described as rupturing each segment (e.g., Ando 1975; Aida 1981; An'naka et al. 2003; Furumura et al. 2011). The segments have been characterized with a fault geometry based on studies of the plate interface along the Nankai Trough, geological surveying, and tsunami simulations. The 1707 Hoei earthquake ruptured from Suruga Bay to the Nankai area and the fault segments across the region ruptured simultaneously (Matsu'ura et al. 2010). Thus, the Hoei earthquake has been considered as representative of the largest earthquake case occurring in the Nankai Trough area.

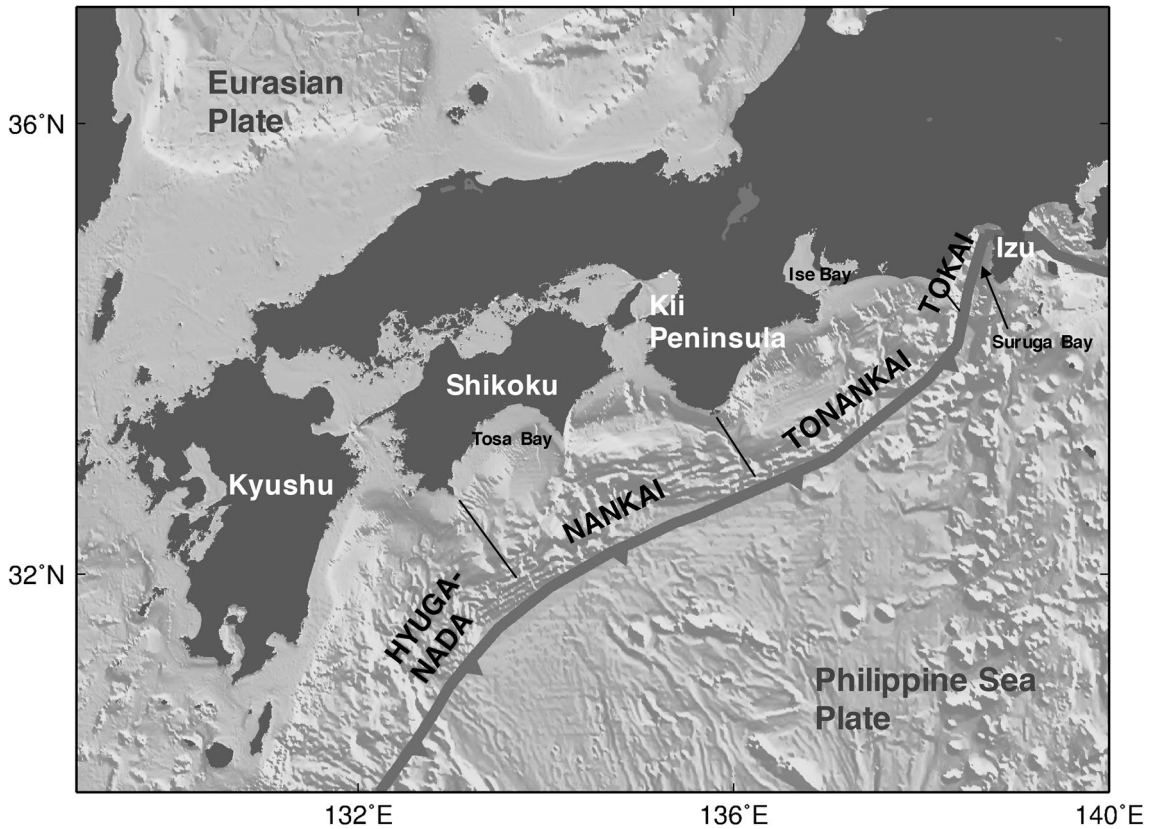

Fig. 2 Bathymetry map of the Nankai Trough area. *Thick gray line* indicates the Nankai Trough where the Philippine Sea Plate is subducting under the Eurasian Plate. The Nankai Trough is divided into four segments: Hyuga-nada, Nankai, Tonankai, and Tokai

Tsuji et al. (2014) reported that a historical Korean document records the 1707 Hoei earthquake tsunami, and the tsunami is also recorded in historic Chinese literature. This indicates that one of the largest earthquakes to have occurred in Japan might have reached both Korea and China. The historical Korean literature suggests the possibility that tsunamis due to potential earthquakes in the Nankai Trough can impact the Korean Peninsula in the future. However, historical records do not provide the details of the propagation process from Japan to Korea, nor do they indicate quantitatively the tsunami height near the coastline of Korea. We used numerical simulation techniques to reproduce the details of tsunamis reported in the historical documents.

We conducted numerical simulations to investigate how tsunamis generated by large earthquakes in the Nankai Trough affect the coastline of Korea. We first analyzed how the tsunami caused by the 1707 Hoei earthquake-affected Korea. We reproduced the tsunami heights and arrival times at the Korean coast using the model of the Hoei earthquake proposed by Furumura et al. (2011). Then, we estimated the tsunamis generated by possible large earthquakes in the Nankai Trough with physically reasonable earthquake scenarios proposed by Hok et al. (2011). We described the characteristics of tsunamis caused by the Nankai Trough earthquakes and the associated risks in Korea.

Description of the 1707 Hoei tsunami in historical Korean and Chinese documents

A historical Korean document called "Tamnaji" containing records of provinces of Jeju Island, located to the south of the Korean Peninsula, describes an observation of waves of abnormal amplitude. The record is dated October 29 and November 4, 1707 (Tsuji et al. 2014). Earthquakes and a volcanic eruption are also recorded around the same date. However, there is no information on the observed height of the abnormal sea waves or its location, making it difficult to assume any details from the document.

In addition, a historical Chinese document called "Huzhou Fu zhi" contains records from the city of Huzhou that state, "Suddenly, the water of the river increased" on October 28, 1707 (Tsuji et al. 2014). The city is located between Lake Taihu and the Qiantang River, and it is not near the coast, so it can be presumed

that the Hoei tsunami traveled up the Yangtze River. Other historical Chinese documents from cities located near the Qiantang River also record that the water level of the river rose rapidly on the same day as the Hoei earthquake occurred, and some documents record that the wave appeared suddenly without any other accompanying event (Wang et al. 2005; Wen et al. 2014).

These historical documents indicate the possibility that a tsunami caused by a large earthquake in the Nankai Trough reached Korea and China. This also suggests potential risks from tsunamis in Korea generated by large earthquakes in the Nankai Trough.

Tsunami simulation of the 1707 Hoei earthquake

Numerical computation of the 1707 Hoei tsunami

We first attempted to examine how the tsunami propagated toward Korea and to identify whether the abnormal wave documented in the historical Korean document was indeed the tsunami from the Hoei earthquake. For numerical computation of the Hoei tsunami, we used the Hoei earthquake source model (Mw 8.8) proposed by Furumura et al. (2011), which was modified from the Hoei source model of An'naka et al. (2003). The fault model of An'naka et al. (2003), consisting of four subfault segments, was an update of the source model of Aida (1981), by taking into account geodetic and geological data from the Nankai Trough, such as depth contours on the surface of the Philippine Sea Plate. Furumura et al. (2011) added an additional segment in the Hyuga-nada area because of recent findings of tsunami-induced oceanic deposits at a seashore in Kyushu, and fault parameters of the fault geometry were assumed to be the same as those for the model of An'naka et al. (2003). Also, the westernmost subfault segment of the model by An'naka et al. (2003) was modified by shortening its length to fit the calculated ground deformation to the observed one. Table 1 shows the source parameters of the five segments model deduced by Furumura et al. (2011). We assumed that the initial tsunami height distribution was equivalent to the vertical seafloor deformation caused by a uniform slip in a fault in a homogeneous half-space. We calculated the vertical seafloor deformation (Fig. 3) using the analytical solution with a Poisson ratio of 0.25 (e.g., Okada 1985, 1992). The tsunami propagation is assumed to be governed by the following nonlinear long-wave equations:

$$\frac{\partial u}{\partial t}+\frac{u}{R_0 cos\varphi}\frac{\partial u}{\partial \lambda}+\frac{v}{R_0}\frac{\partial u}{\partial \varphi}+\frac{g_0}{R_0 cos\varphi}\frac{\partial \eta}{\partial \lambda}=-\frac{g_0 n_0^2}{(h+\eta)^{\frac{1}{3}}}\frac{\sqrt{u^2+v^2}}{h+\eta}u \tag{1}$$

$$\frac{\partial v}{\partial t}+\frac{u}{R_0 cos\varphi}\frac{\partial v}{\partial \lambda}+\frac{v}{R_0}\frac{\partial v}{\partial \varphi}+\frac{g_0}{R_0}\frac{\partial \eta}{\partial \varphi}=-\frac{g_0 n_0^2}{(h+\eta)^{1/3}}\frac{\sqrt{u^2+v^2}}{h+\eta}v \tag{2}$$

$$\frac{\partial \eta}{\partial t}+\frac{1}{R_0 cos\varphi}\frac{\partial}{\partial \lambda}\{u(h+\eta)\}+\frac{1}{R_0 cos\varphi}\frac{\partial}{\partial \varphi}\{v(h+\eta)cos\varphi\}=0 \tag{3}$$

where R_0 is equal to the Earth's radius, λ is longitude, and φ is latitude. The parameters u and v are the vertically averaged horizontal velocity components in the east and north directions, respectively. The parameter η is tsunami height, h is water depth, and g_0 is the average acceleration of gravity on the earth surface. The Manning's roughness coefficient n_0 of 0.03 s/m$^{1/3}$ was employed for the entire simulation area (e.g., Satake 1995). Inundation was represented in the simulation by changing the boundary between land and sea according to the water flow into the land area (e.g., Iwasaki and Mano 1979; Saito et al. 2014). We do not consider wave breaking or Coriolis forces.

We numerically solved the nonlinear long-wave equation using a staggered leap-frog finite difference method. The simulation area included the Nankai Trough region, the south coast of the Korean Peninsula, and the East Sea of China (Fig. 4a). Figure 4b shows the topography near Jeju Island, and Fig. 4c shows the coastlines of the Korean Peninsula and Jeju Island. We used 30 arc-second bathymetric data taken from the General Bathymetric Chart of the Oceans (GEBCO) database hosted by the British Oceanographic Data Centre (BODC; GEBCO_2014 Grid, available for download at http://www.gebco.net, 2014). A total simulation time of 15 h was required to examine the

Table 1 Fault parameters of the 1707 Hoei earthquake deduced by Furumura et al. (2011)

Segment	Fault location[a] Latitude (°N)/Longitude (°E)	Length (km)	Width (km)	Depth (km)	Strike (°)	Dip (°)	Rake (°)	Slip (m)
N1	35.120/138.706	120	50	6.4	193	20	71	5.6
N2	33.823/138.235	205	100	4.1	246	10	113	7.0
N3	33.006/136.074	155	100	7.8	251	12	113	5.6
N4′	32.614/134.481	135	120	10.1	250	8	113	9.2
N5′	32.200/133.130	70	80	10.0	250	8	118	9.2

[a] The fault location is east corner of each subfault

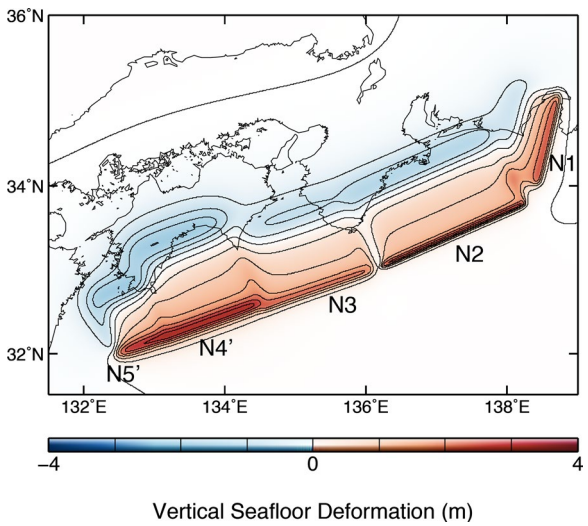

Fig. 3 Vertical seafloor deformation of the 1707 Hoei earthquake source model by Furumura (2011). The *contour line* interval is 0.5 m. *Red* and *blue colors* indicate uplift and subsidence, respectively

tsunami arrivals at the eastern coastline of China, and the time step was set to 1 s for computational stability.

Results of the 1707 Hoei tsunami simulation

Figure 5 shows snapshots of the calculated tsunami height distribution at elapsed times (T) of 0, 60, 120, 180, 200, and 300 min after occurrence of the Hoei earthquake. The initial tsunami height is shown in Fig. 5a ($T = 0$ min) with a large amplitude (~3.5 m) near the Nankai Trough. The tsunami turned around Kyushu at $T \sim 60$ min, and a tsunami of large amplitude propagated to the Pacific Ocean (Fig. 5b). The tsunami passed the Okinawa region at $T = 120$ min (Fig. 5c). At this point, the wave was still turning around Kyushu and its amplitude decreased. The wave traveled toward Korea at 180 min (Fig. 5d). Figure 5e shows that the tsunami reached Jeju Island at T = 200 min and arrived at the southern coast of the Korean Peninsula at $T = 300$ min (Fig. 5f).

Figure 6 shows the distribution of numerically simulated maximum tsunami heights along the coastlines of southern Korea and Jeju Island. Points showing the highest amplitudes along both coastlines are marked as H2 and H3 in the figure, and the heights are 0.47 and 0.45 m, respectively, although these values can change more or less if a coarser grid spacing of 1-min bathymetry data is used. Generally, it would be difficult to predict the maximum height tsunami values exactly. The heights are mostly distributed between 0.1 and 0.3 m along the coastlines of both regions. We confirmed that this distribution does not change significantly if the grid spacing is changed from 1 min to 30 s. Also, larger tsunami amplitudes were generally observed between headlands and embayments. In contrast, we obtained very low tsunami amplitudes of <0.1 m along the northern coast of Jeju Island.

Figure 7 shows the tsunami waveforms, or the temporal change in sea surface height, at points P1, P2, P3, and P4 indicated in Fig. 6. Our results show that the first tsunami peak is not necessarily the maximum height. The waveform at point P1 (Fig. 7a) shows that the wave of the first peak arrived at an elapsed time of 310 min, and then the maximum height arrived ~ 400 min after the arrival of the first peak. The waveform at point P2 (Fig. 7b) shows a similar result to that of the first peak, and the maximum peaks were recorded at elapsed times of 330 min and 580 min, respectively. Figure 7c, d shows records at P3 and P4, respectively, on the coastline of Jeju and shows higher-frequency components than waveforms at P1 and P2 (Fig. 7a, b). At P4, the highest tsunami arrived 10 h (600 min) after the arrival of the first peak.

We found that the tsunami propagation time to China took longer than that to Korea, and the tsunami reaching China had a higher amplitude. Figure 8a shows the tsunami height distribution at $T = 180$ min from occurrence of the earthquake. At the same elapsed time, the tsunamis of box A pass through a region of shallower sea depths (50 m–100 m), while the waves of box B propagate through a deeper region (about 150 m). Hence, the tsunami waves in box B that traveled toward Korea propagated slightly faster than the tsunami waves in box A, which propagated to the eastern coast of China. The tsunami traveling toward China (box A) propagated with large amplitude until it reached the Shanghai area. Figure 9 shows waveforms from virtual stations on the eastern sea of China, and the stations are located on different sea depths (Fig. 8a). It clearly shows that even though the travel distance increases, meaning the tsunami should lose energy due to geometric spreading of the wave front and bottom friction, the tsunami height increases because of decreasing sea depth. This effect was also seen in previous studies of tsunami waves propagating in the eastern sea of China (Kim et al. 2013; Wen et al. 2014). Figure 8b shows the spatial distribution of maximum tsunami heights near the Chinese coast showing that a larger-amplitude tsunami (~0.7 m) reached the coast of China than the tsunami near Korea. These results from our simulations are consistent with the historical Chinese records.

Tsunami simulation of Nankai Trough large earthquakes

Anticipated earthquake scenarios in the Nankai Trough

The historical records imply that potential tsunamis generated in the Nankai Trough region could affect the

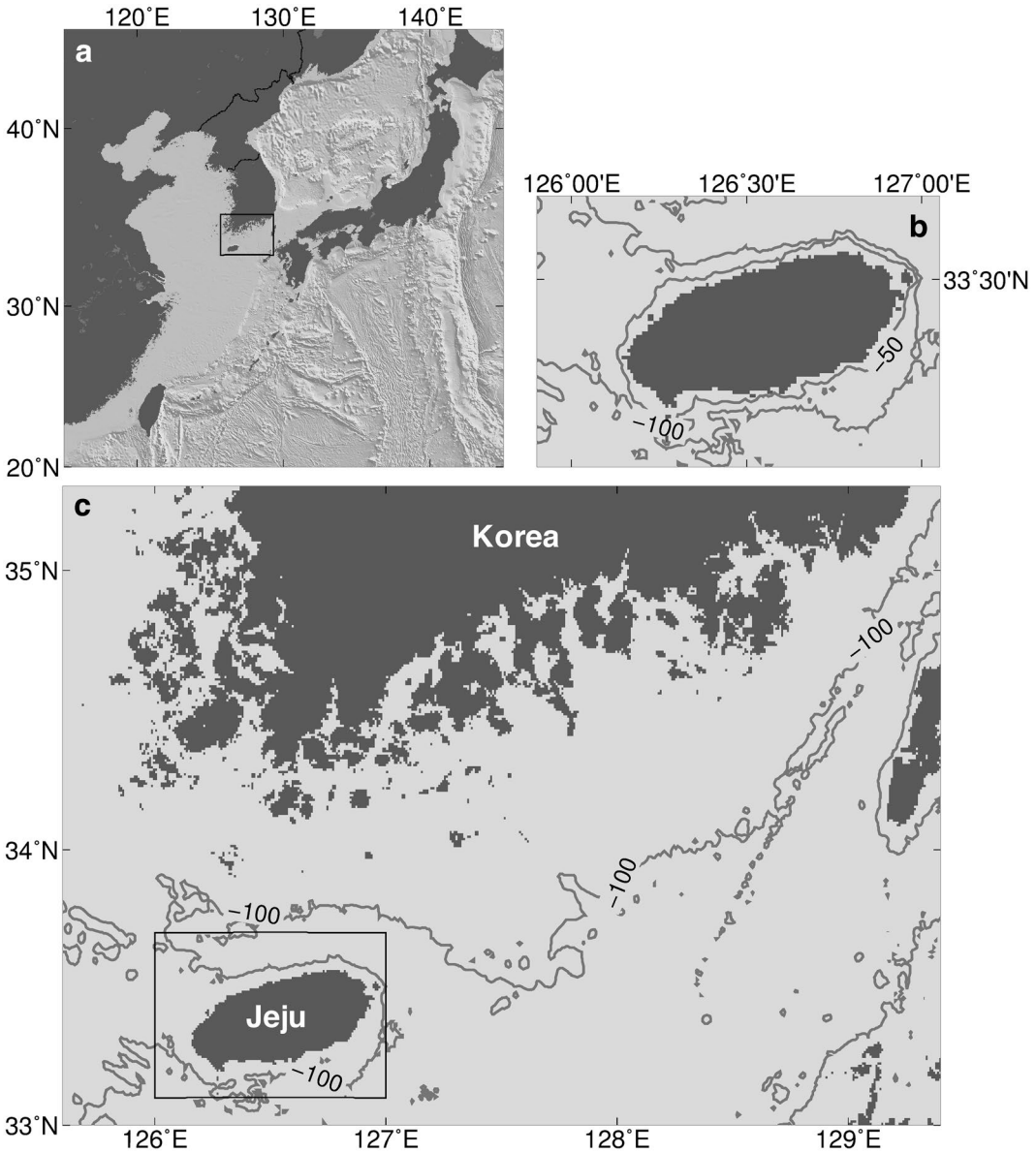

Fig. 4 Maps of the areas of tsunami simulation. **a** Entire area of tsunami simulation. *Rectangular box* shows the region enlarged in **c**. **b** Topography around Jeju Island. **c** Coastlines of the Korean Peninsula and Jeju Island

Korean Peninsula in the future. To predict future tsunami disasters, we conducted tsunami simulations for potential Nankai earthquakes.

To assess the potential tsunami hazard, it is crucial to apply physically reliable earthquake models for tsunami simulation to obtain more realistic tsunamis. In this study, the earthquake rupture scenarios by Hok et al. (2011) are used for the prediction of the future Hoei-like earthquake. The advantage of using Hok et al. (2011) compared with other studies is that it includes the current deformation rate of the plate, and the computations include a dynamic term in the rupture propagation which is ignored in most studies.

To compute dynamic rupture scenarios, Hok et al. (2011) used a boundary integral equation method developed by Hok and Fukuyama (2011). Hok et al. (2011) used the three-dimensional geometry of the plate interface model of Hashimoto et al. (2004) to capture features of fault geometry and made a fault interface composed of 13,385 triangular elements with 7400 triangular elements at the free surface. These fault elements are used to simulate dynamic rupture earthquakes. The initial stress

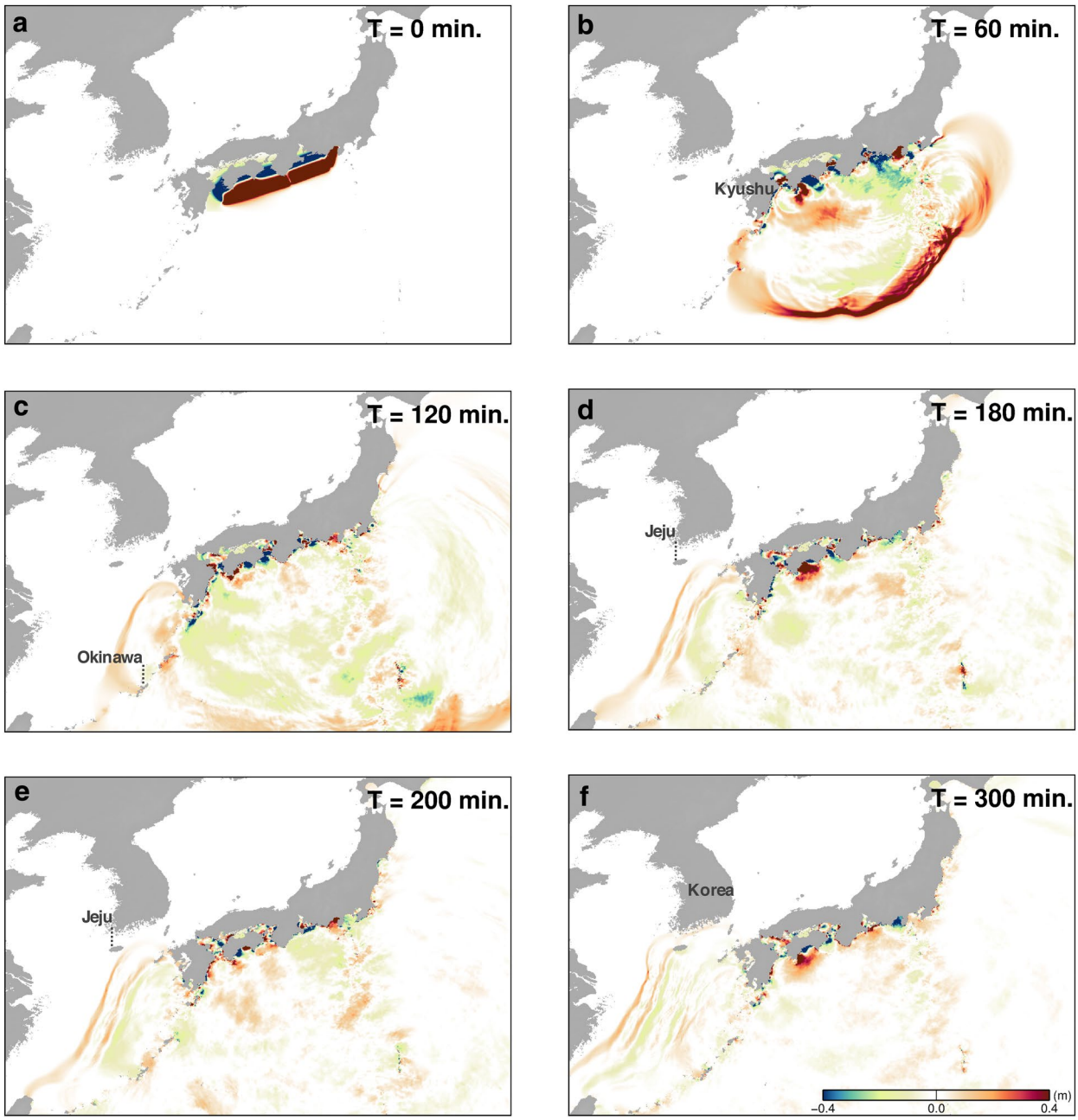

Fig. 5 Simulated sea surface height distribution for propagation of the 1707 Hoei tsunami. The elapsed times of **a** $T = 0$ min (initial tsunami height distribution), **b** $T = 60$ min, **c** $T = 120$ min, **d** $T = 180$ min, **e** $T = 200$ min, and **f** $T = 300$ min after occurrence of the Hoei earthquake. *Colors* indicate sea level heights, whose scale is shown in the *bottom right* of *panel* **f**

distribution is obtained from the slip-deficit rate. Hashimoto et al. (2009) deduced the slip-deficit rate distribution along the Nankai Trough using GPS Earth Observation Network (GEONET) data for 4 years, which Hok et al. (2011) used to calculate the accumulated slip-deficit rate for 100 years. Stress drop is estimated from the slip distribution which is derived from the slip-deficit distribution.

Since the scenarios by Hok et al. (2011) were obtained by a fully elastodynamic simulation and physical parameters from direct and indirect observations, Hok et al. (2011) constructed various large potential interplate earthquakes caused by the release of stress that has been accumulated in and around the focal area (the Nankai subduction zone). We employed two scenarios from Hok et al. (2011) and two

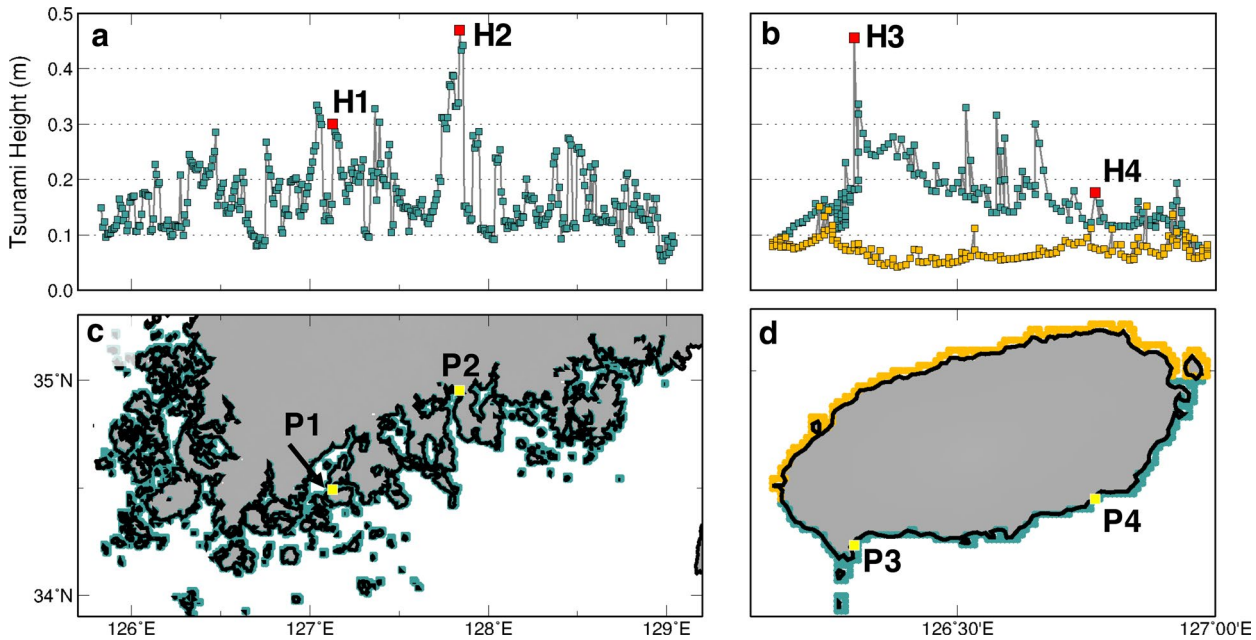

Fig. 6 Simulated maximum tsunami height along coastlines. Panels **a**, **b** show the maximum tsunami height distributions along the coastlines of the southern Korean Peninsula and Jeju Island, respectively. H1, H2, H3, and H4 in these panels represent the tsunami heights at points P1, P2, P3, and P4 in **c** and **d**, respectively. Panels **c**, **d** show the coastlines corresponding to **a** and **b**, respectively. In panel **d**, each *color* corresponds to the *colors* of the height distributions in **b**

additional scenarios which were constructed in the same way with different parameters (Table 2). Consequently, we used four scenarios whose moment magnitudes ranged from 8.5 to 8.6, which we refer to in this paper as SC01, SC02, SC03, and SC04 (Fig. 10).

In scenario SC01 (Mw 8.56), the rupture area included the Hyuga-nada area and the region off Shikoku Island, and rupture started at the western edge of the Nankai area. Despite the high slip-deficit rate observed in this region, the amount of slip was lower than other models. This is because a large slip-weakening distance was assumed in Hok et al. (2011) to simulate slow slip in the Hyuga-nada segment. A large slip-weakening distance makes it difficult for coseismic slip to occur during dynamic simulations following the slip-weakening friction law. SC02 had the smallest moment magnitude (Mw 8.5) among the four models, whereas the maximum slip was much larger than for SC01. The rupture initiated at the tip of the Kii Peninsula, which is the same hypocenter as that of the 1946 Nankai earthquake. SC03 (Mw 8.61) ruptured the entire Nankai-Tonankai area as a single event with the rupture initiating at the western edge of the Nankai segment. However, in this model the rupture did not propagate to the Tokai area, which is commonly thought to be the initial rupture point of the Hoei earthquake. Hok et al. (2011) reported that they did not include the Tokai area in their study, but they considered the eastern edge of the Tonankai region as one of the initial points in their dynamic simulation. In SC04 (Mw 8.65), the rupture started from Ise Bay and propagated to the western side of the Nankai region. The dimensions of the rupture area were similar to those of SC03, but the initial rupture started at Ise Bay. In terms of the estimated rupture area and moment magnitude, we believe SC04 is the closest model to an anticipated Hoei earthquake among the four scenarios.

Before estimating the vertical seafloor deformation of each scenario, we adjusted the grid locations. The earthquake scenarios by Hok et al. (2011) are composed of 13,385 triangular fault elements whose collocation points are located at an interval of 4 km, and each element has an area of 16 km^2 when projected to the free surface. However, we used the analytical solution for a rectangular fault (Okada 1985, 1992) which required us to modify the fault elements. To accommodate the differences between the fault geometry, we applied a piecewise linear interpolation with an interval of 4 km for rectangular fault elements of 4 km $\times$ 4 km. We then calculated the sea bottom deformation by representing the heterogeneous slip model by numerous small rectangular faults and used the same method for the numerical tsunami computations as that of the Hoei tsunami simulation.

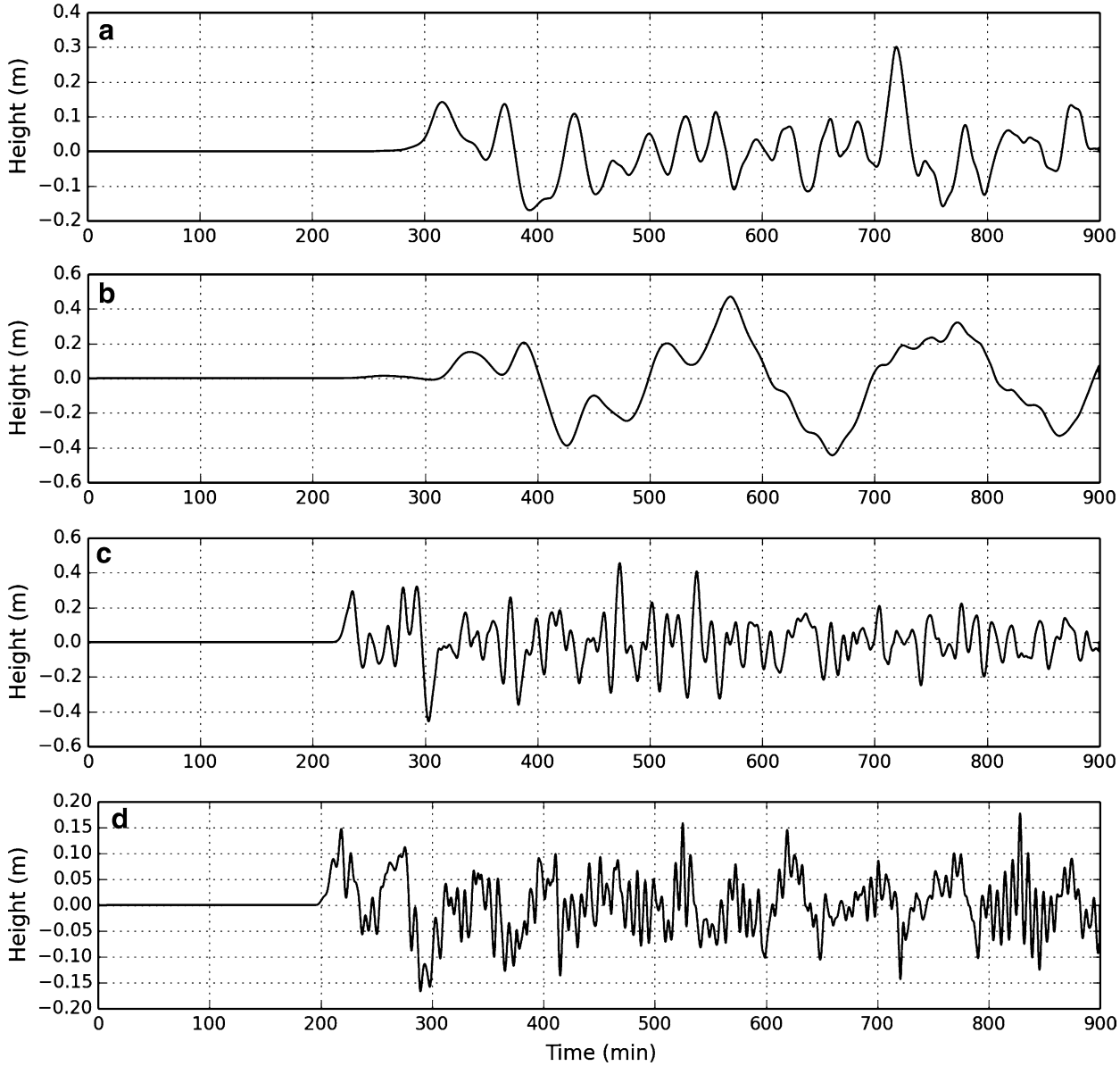

Fig. 7 Simulated tsunami waveforms of the Hoei earthquake. The waveforms **a**, **b**, **c**, and **d** are for the points P1, P2, P3, and P4 in Fig. 6, respectively

Tsunamis on the Korean coast

By computing tsunamis using physically reasonable scenarios of the Nankai Trough region, we obtained tsunami height distributions along the southern coastline of the Korean Peninsula and the southern coast of Jeju Island (Fig. 11). The distributions were similar among the four models. The maximum tsunami heights among the four scenarios were about 0.4 and 0.3 m along the Korean Peninsula and the coastlines of Jeju, respectively. The tsunami heights resulting from SC01 showed larger amplitude on the southern coastline of the Korean Peninsula than the other models, despite the absence of significant slip. The larger amplitude could be explained by the rupture area being closer to Korea. In contrast, SC02 had the highest tsunami heights around Jeju Island. SC03 showed an analogous pattern to SC01, which had larger amplitude along the southern Korean Peninsula and smaller amplitude at Jeju. SC04, which was the model with the largest magnitude, showed similar results to SC02. The tsunami height distributions were generally similar among the four scenarios because the sizes or the moment magnitudes of the four rupture models were almost identical.

Then, we compared the tsunami simulation results of the Hoei earthquake source model and the four scenarios (Fig. 12). The average maximum tsunami height of the four scenarios around Jeju Island showed similar patterns

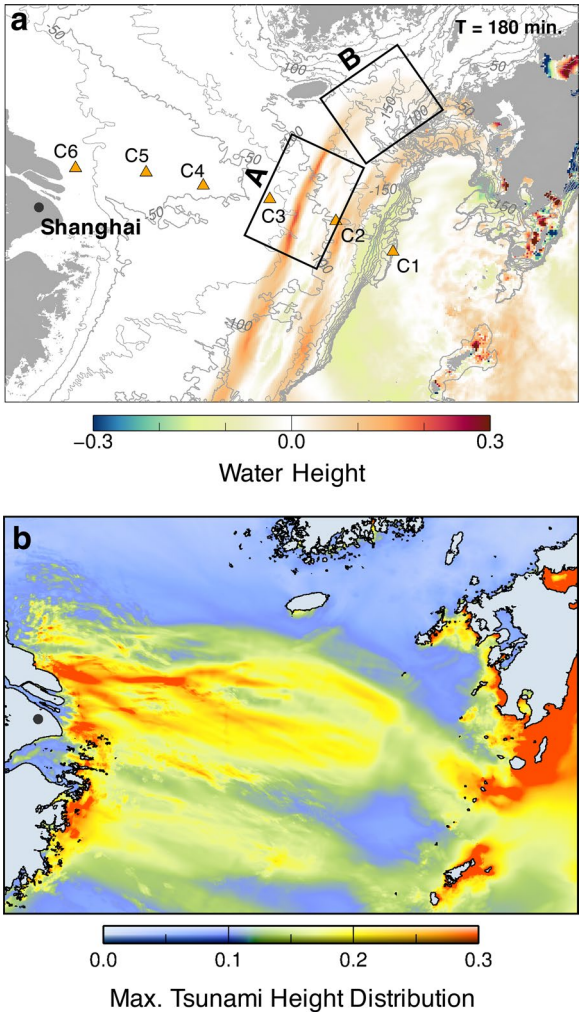

Fig. 8 Simulated tsunami height distributions of the Hoei earthquake. **a** Snapshot of the simulated tsunami height at the elapsed time of 180 min after occurrence of the Hoei earthquake. The *yellow triangle symbols* indicate virtual stations. The interval of depth contour is 25 m. **b** Maximum tsunami height distribution around Korea and China. Scales for both figures are in units of meters

to the maximum height distribution of the Hoei tsunami, despite the fact that they had different slip distributions. The tsunami amplitudes derived from the Hoei earthquake were twofold or threefold larger than the average amplitudes of the scenarios, because the seismic moment of the Hoei earthquake was twofold to threefold larger than those of the four scenarios.

Discussion

The Hoei earthquake tsunami and historical documentation in Korea

Our simulation results using the Hoei earthquake source model produced a maximum tsunami height along the southern coast of Jeju Island of ~0.5 m, whereas it was ~0.15 m along the northern coast, the most populated area of Jeju Island. This implies that the abnormal sea wave recorded in the historical Korean document was the Hoei earthquake tsunami. However, considering that the northern coast of Jeju Island was more populated, a tsunami of ~0.15 m height might have been too small to be recognized by people. Hence, it might be difficult to conclude that the abnormal sea waves described in the historical document were in fact a tsunami originating directly from the Hoei earthquake. Our simulation indicates that the abnormal sea waves described in a historical Korean document could be the tsunami from the Hoei earthquake, or it could also be a tsunami produced from a secondary source such as a submarine landslide induced by the strong ground motion of the Hoei earthquake. Landslides are often reported when large earthquakes have occurred and can generate large tsunamis locally (e.g., Bryant 2014). However, it is uncertain that landslide-generated tsunamis occurred near Kyushu Island or Jeju Island after the Hoei earthquake. Examining the possibility of a landslide tsunami near Jeju Island is not straightforward, but presents a topic for possible future study.

Variation in the maximum tsunami height due to the difference in the stress drop

We consider that the physics-based scenarios in our analysis are probable in the future but do not represent the maximum earthquake that could possibly occur in the Nankai Trough region (Hyodo et al. 2014). To consider the effects of a larger magnitude earthquake, we increased the stress drop of SC03 by a factor of two and three compared with the original dynamic simulation. Hok et al. (2011) assumed that the stress accumulation could be estimated based on the distribution of the total amount of slip deficit for 100 years. Thus, if we assume that the slip deficit has accumulated for 200 or 300 years, it would create a twofold or threefold amount of slip in the same rupture area. Based on this assumption, we obtained two additional earthquake models: one for 200 years of slip-deficit accumulation characterized by the same moment magnitude as the Hoei earthquake (Mw 8.8) and the other (300 years of slip-deficit accumulation) with an Mw of 8.9. We refer to these models as SC03_A and SC03_B, respectively. Tsunami simulations were performed using these two models with the same methods employed in the previous sections.

We compared the maximum tsunami heights of SC03_A and SC03_B with those of the Hoei earthquake source model (Fig. 13). The comparison showed similar patterns among the three models along the Korean coast. The amplitude distribution of Model SC03_A (Mw 8.8) was 0.1–0.2 m larger than that of the Hoei model, and

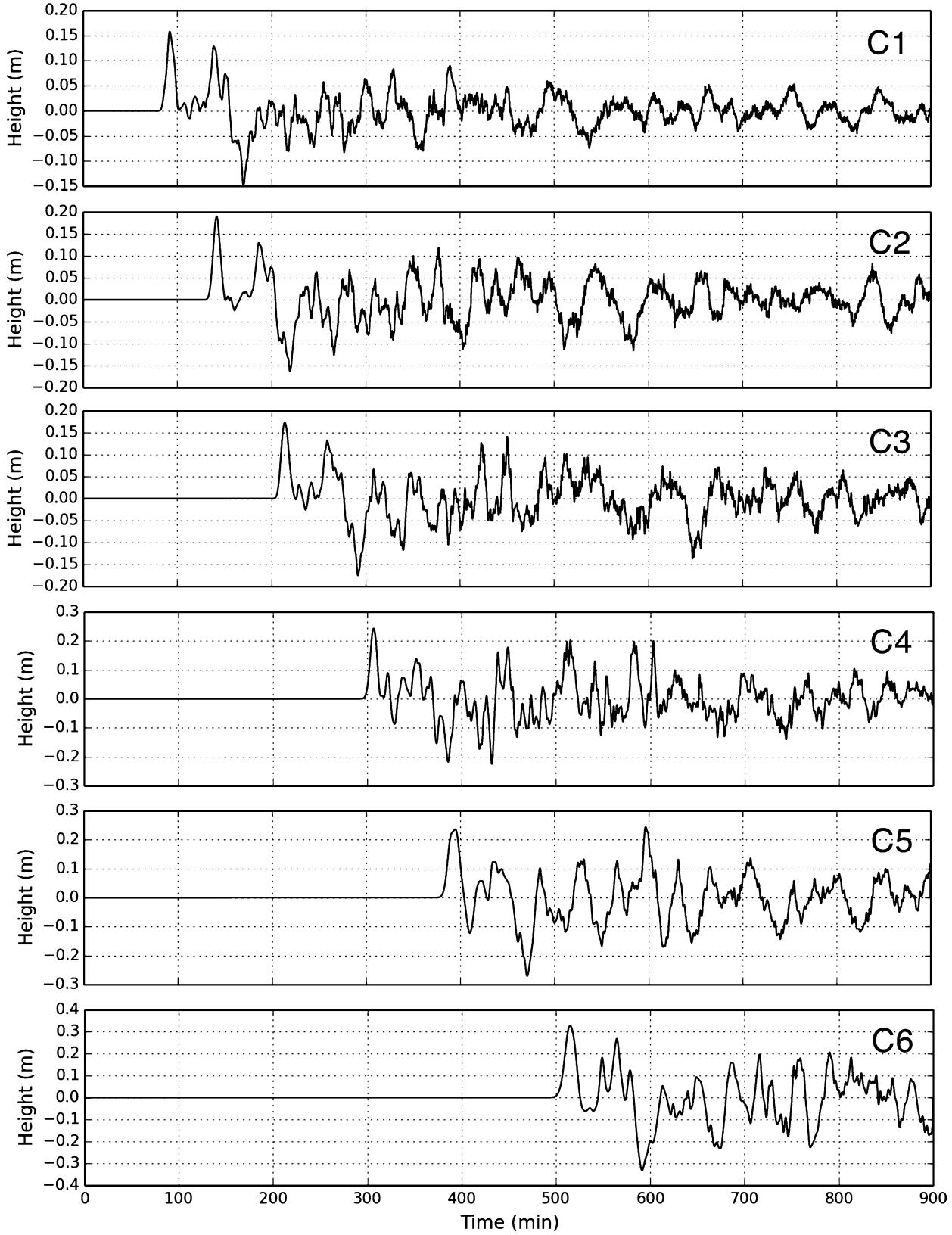

Fig. 9 Simulated tsunami waveforms on the eastern sea of China. The waveforms are estimated at the virtual stations located on the eastern Chinese coast (Fig. 8a)

Table 2 Parameters of anticipated scenarios

Model	Medium	k^a (%)	Initiation	Strength	Final size	Name in Hok et al. (2011)
SC01	Half-space	–[b]	Western edge of Nankai	Uniform[c]	Hyuga-nada and Nankai	–
SC02	Half-space	20	1946 Nankai hypocenter	Uniform	Nankai	–
SC03	Half-space	20	Western edge of Nankai	Uniform	Nankai and Tonankai	H4
SC04	Full-space	25	Eastern edge of Tonankai	Step[d]	Tonankai and Nankai	B3

[a] *k* is the scaling factor of slip-weakening distance

[b] Constant slip-weakening distance is used

[c] Uniform stands for the model whose static shear strength is uniform and is set at 10.5 MPa

[d] Step indicates the model where the static shear strength is 10.5 MPa in the western part and 9 MPa in the eastern part; the boundary is located southwest of the Kii Peninsula

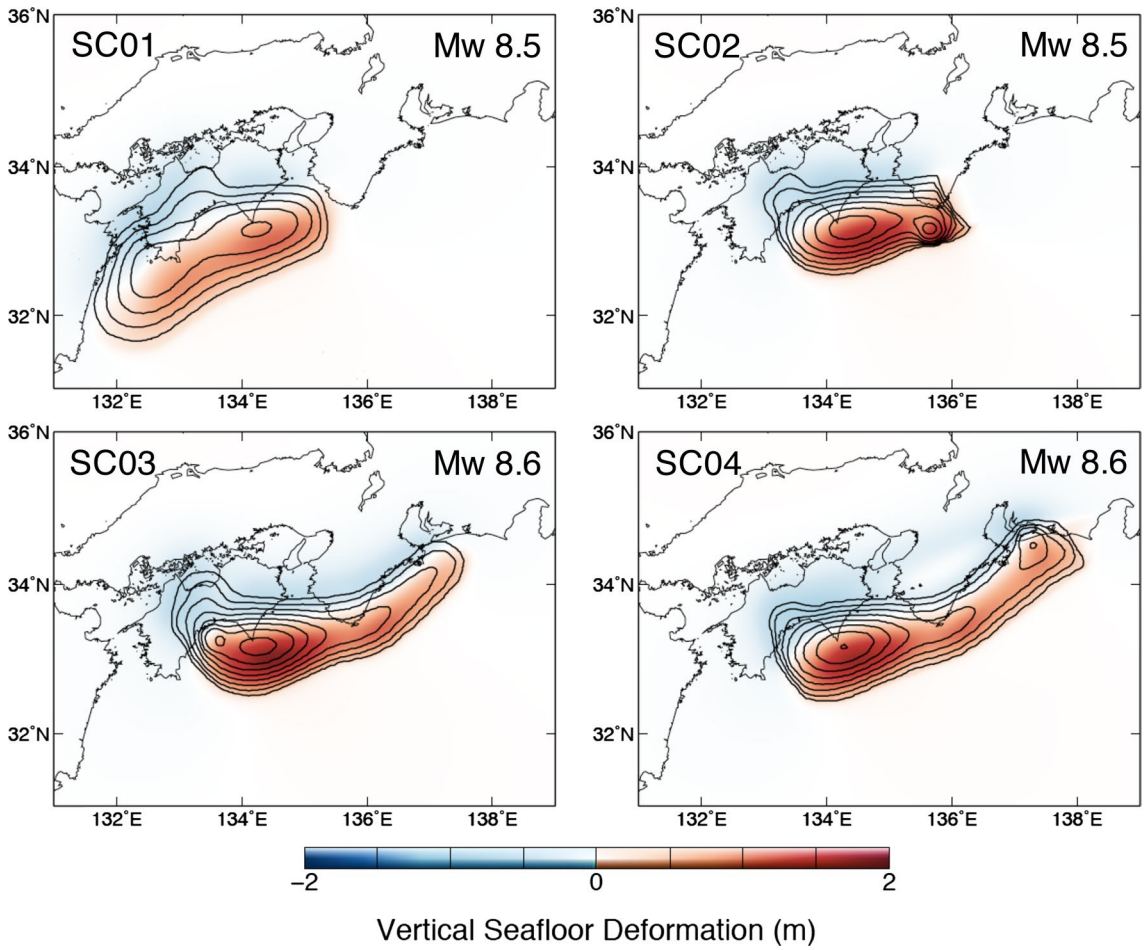

Fig. 10 *Vertical* seafloor deformation for the anticipated earthquake scenarios. The four earthquake models SC01, SC02, SC03, and SC04 were constructed by Hok et al. (2011). *Red* and *blue colors* indicate uplift and subsidence on the sea *bottom*, respectively. The slip on the fault is contoured at 1-m intervals

Model SC03_B (Mw 8.9) had an amplitude distribution of 0.2–0.4 m larger than the Hoei model. The highest tsunami amplitude of SC03_B was ~0.9 m along the southern coastline of Korean Peninsula.

Risks associated with Nankai Trough earthquake tsunamis on the Korean coast

Our simulation results from the Hoei earthquake model and the anticipated earthquake models showed that the

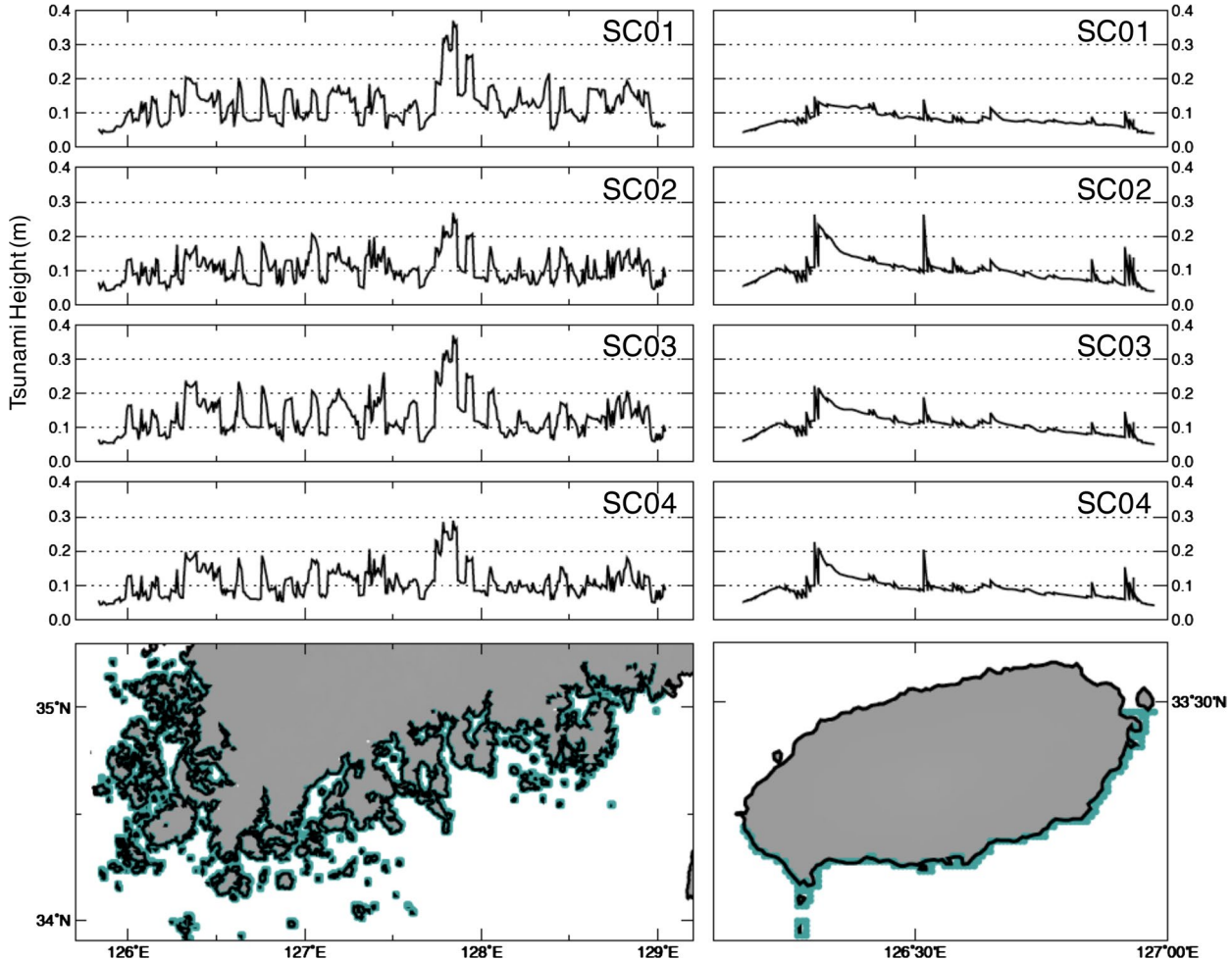

Fig. 11 Maximum tsunami height distributions for the four anticipated Nankai earthquake scenarios. The upper four rows show the simulation results using the models SC01, SC02, SC03, and SC04

maximum tsunami height along the Korean coast was <0.5 m. The tsunami would not be life-threatening, but it would disrupt economic activities such as fish farming. For example, Imai et al. (2010) report small-amplitude far-field tsunamis (<0.3 m) disrupted fish farming.

We also note that the arrival of the first tsunami does not always correspond to the maximum height. The maximum height possibly arrives 300–600 min after the first tsunami. The tsunami maintains relatively large amplitudes for a significant period from the arrival of the first peak to the arrival of the wave of maximum height (Fig. 7). It is important to take this characteristic of long duration of large-amplitude waves into account for planning tsunami hazard mitigation strategies in Korea.

Our simulation clearly indicates that tsunamis from the Nankai Trough earthquakes arrive at the Korean coast by passing offshore of Kyushu. Thus, it would be useful to install offshore tsunami gauges between Korea and Kyushu and analyze the records using a data assimilation analysis to forecast tsunami heights and arrival times on the Korean coast. However, there are also limitations in the prediction of tsunamis because we cannot neglect the possibility that strong ground motion can trigger a submarine landslide near the Korean coast that acts as a secondary tsunami source. If a landslide occurs near the coast, locally large-amplitude tsunamis can arrive at the coast earlier than we would expect from a data assimilation analysis.

Conclusion

We reproduced the historical tsunami generated by the 1707 Hoei earthquake using a simulation with the fault model proposed by Furumura et al. (2011), and estimated its propagation process and wave height on the coastlines

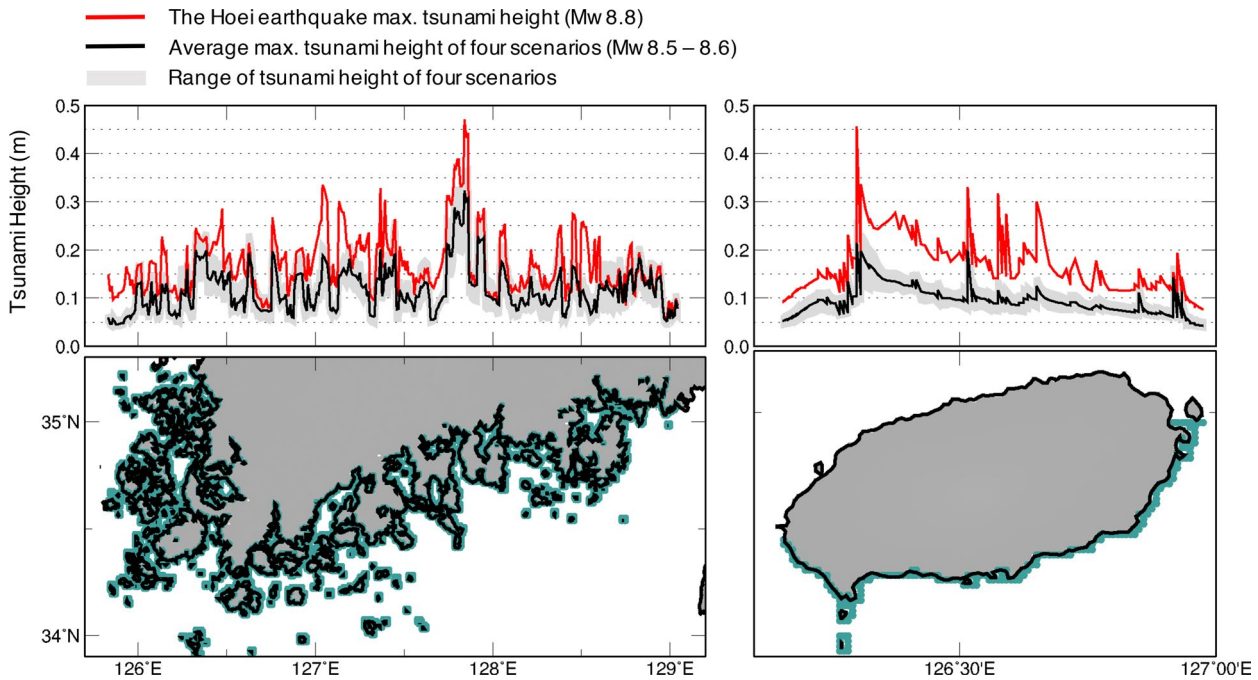

Fig. 12 Comparison between simulation results of the Hoei earthquake source model and the four scenarios. Maximum tsunami height distributions for the 1707 Hoei earthquake source model (*red*) and the four anticipated Nankai earthquake scenarios (*black and gray*)

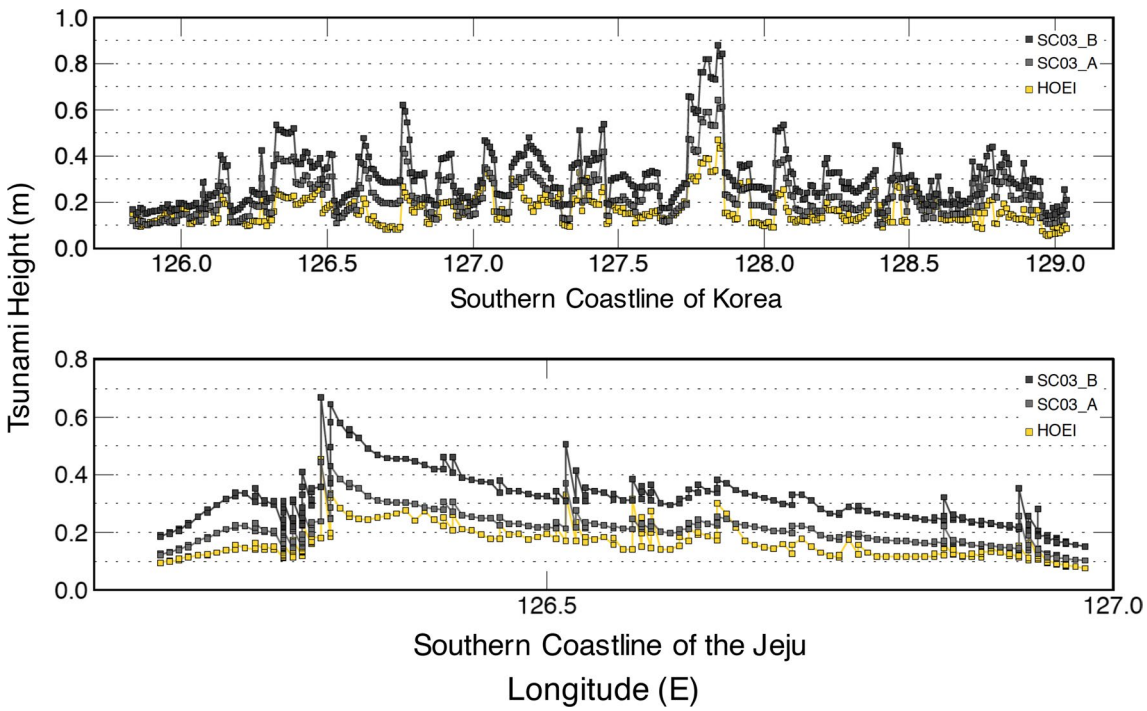

Fig. 13 Tsunami height distributions for different values of the stress drop. Maximum tsunami height distributions for different values of stress drop in *light gray* and *dark gray*. SC03_A and SC03_B have twofold and threefold greater stress drop compared with the scenario SC03, respectively. The maximum height distribution of the Hoei earthquake is shown in *yellow*

of Korea. We found that the Hoei earthquake (Mw 8.8) tsunami reached Korea about 200 min after the occurrence of the earthquake. The maximum tsunami height was ~0.5 m along the southern coast of Jeju Island and the Korean Peninsula, whereas the height was less than 0.15 m along the northern coast of Jeju Island, the most populated area on Jeju Island. The maximum tsunami height arrived about 600 min after the first peak arrived, which resulted in a tsunami of long duration. In addition, we conducted tsunami simulations using scenarios of physically reasonable anticipated earthquakes in the Nankai Trough region. We obtained a maximum tsunami height of ~0.4 m among the four scenarios along the Korean coast for the anticipated earthquakes (Mw 8.5–8.6). To evaluate larger possible tsunamis, we increased the stress drop in the earthquake model by twofold and threefold and constructed the scenarios for earthquakes of Mw 8.8 and 8.9. The tsunami height increased by 0.1–0.4 m compared to the Hoei earthquake. Tsunamis produced by large Nankai Trough earthquakes would not be devastating to Korea; however, the effect of larger earthquakes still needs to be considered.

Authors' contributions

SK carried out the simulation studies and produced a draft of the manuscript. TS and EF carried out the setup of earthquake models and tsunami simulation strategy. TK conceived of the study and carried out the historical documentary studies. All authors read and approved the final manuscript.

Author details

[1] Department of Earth and Environmental Sciences, Pukyong National University, 45 Yongso-ro, Nam-gu, Busan 48513, Republic of Korea. [2] National Research Institute for Earth Science and Disaster Prevention, 3-1 Tennodai, Tsukuba, Ibaraki 305-006, Japan.

Acknowledgements

We thank the editor and anonymous reviewers for their constructive comments for improving the manuscript. This work was funded by the Korea Meteorological Administration Research and Development Program under Grant KMIPA 2015-7120. Part of this research was supported by the National Research Institute for Earth Science and Disaster Prevention (NIED) under the project entitled "Development of the Earthquake Activity Monitoring and Forecasting." SB is grateful to National Research Foundation of Korea (NRF), Japan International Science and Technology Exchange Center (JISTEC), and Japan–Korea Industrial Technology Co-Operation Foundation for their support in her visiting NIED.

Competing interests

The authors declare that they have no competing interests.

Received: 4 February 2016 Accepted: 6 April 2016
Published online: 23 April 2016

References

Aida I (1981) Numerical experiments for the tsunamis generated off the coast of the Nankaido district. Bull Earthq Res Inst Univ Tokyo 56:713–730 **(in Japanese with English abstract)**

An'naka T, Inagaki K, Tanaka H, Yanagisawa K (2003) Characteristics of great earthquakes along the Nankai Trough based on numerical tsunami simulation. Jpn Soc Civil Eng J Earthq Eng [CD-ROM] 27, article 307 **(in Japanese)**

Ando M (1975) Source mechanisms and tectonic significance of historical earthquakes along the Nankai Trough, Japan. Tectonophysics 27:119–140

Bryant E (2014) Tsunami: the underrated hazard, 3rd edn. Springer, Cham

Fukuyama E, Irikura K (1986) Rupture process of the 1983 Japan Sea (Akita-Oki) earthquake using a waveform inversion method. Bull Seismol Soc Am 76:1623–1640

Furumura T, Imai K, Maeda T (2011) A revised tsunami source model for the 1707 Hoei earthquake and simulation of tsunami inundation of Ryujin Lake, Kyushu, Japan. J Geophys Res 116:B02308. doi:10.1029/2010JB007918

Hashimoto C, Fukui K, Matsu'ura M (2004) 3-D modelling of plate interfaces and numerical simulation of long-term crustal deformation in and around Japan. Pure Appl Geophys 161:2053–2068

Hashimoto C, Noda A, Sagiya T, Matsu'ura M (2009) Interplate seismogenic zones along the Kuril-Japan trench inferred from GPS data inversion. Nat Geosci 2:141–144. doi:10.1038/ngeo421

Hok S, Fukuyama E (2011) A new BIEM for rupture dynamics in half-space and its application to the 2008 Iwate–Miyagi Nairiku earthquake. Geophys J Int 184(1):301–324. doi:10.1111/j.1365-246X.2010.04835.x

Hok S, Fukuyama E, Hashimoto C (2011) Dynamic rupture scenarios of anticipated Nankai–Tonankai earthquakes, southwest Japan. J Geophys Res 116:B12319. doi:10.1029/2011JB008492

Hyodo M, Hori T, Ando K, Baba T (2014) The possibility of deeper or shallower extent of the source area of Nankai Trough earthquakes based on the 1707 Hoei tsunami heights along the Pacific and Seto Inland Sea coasts, southwest Japan. Earth Planets Space 66:123. doi:10.1186/1880-5981-66-123

Imai K, Namegaya Y, Tsuji Y, Fujii Y, Ando R, Komatsubara J, Komatsubara T, Horikawa H, Miyachi Y, Matsyama M, Yoshii T, Ishibe T, Satake K, Nishiyama A, Harada O, Shigihara Y, Shigihara Y, Fujima K (2010) Field survey for tsunami trace height along the coasts of the Kanto and Tokai districts from the 2010 Chile Earthquake. J Jpn Soc Civ Eng Ser B2 (Coast Eng) 66(1):1351–1355 **(in Japanese with English abstract)**

Ishibashi K, Satake K (1998) Problems on forecasting great earthquakes in the subduction zones around Japan by means of paleoseismology. J Seismol Soc Jpn 50:1–21 **(in Japanese with English abstract)**

Iwasaki T, Mano A (1979) Two-dimensional numerical computation of tsunami run-ups in the Eulerian description. In: Proceedings of the Japanese conference on coastal engineering 26, pp 70–74, Kagoshima University, Kagoshima, 20 Nov 1979

Kim KO, Jung KT, Choi BH (2013) Propagation of a tsunami wave generated by an earthquake in the Nankai Trough onto the South Korean coast. In: Conley DC, Masselink G, Russell PE, O'Hare TJ (eds) Proceedings of the 12th International Coastal Symposium, Plymouth, April 2013. Journal of Coastal Research, Special Issue No. 65, pp 278–283

Kumagai H (1996) Time sequence and the recurrence models for large earthquakes along the Nankai Trough revisited. Geophys Res Lett 23:1139–1142

Matsu'ura RS, Nakamura M, Karakama I (2010) New proposal of the focal area for 1707 Hoei earthquake. In: Paper presented at fall meeting of the seismological society of Japan, International Conference Center Hiroshima, Hiroshima, 27–29 Oct 2010

Okada Y (1985) Surface deformation due to shear and tensile faults in a half-space. Bull Seismol Soc Am 75:1135–1154

Okada Y (1992) Internal deformation due to shear and tensile faults in a half-space. Bull Seismol Soc Am 82:1018–1040

Parsons T, Console R, Falcone G, Murru M, Yamashina K (2012) Comparison of characteristic and Gutenberg–Richter models for time-dependent $M \geq 7.9$ earthquake probability in the Nankai–Tokai subduction, Japan. Geophys J Int 190:1673–1688

Saito T, Inazu D, Miyoshi T, Hino R (2014) Dispersion and nonlinear effects in the 2011 Tohoku-oki earthquake tsunami. J Geophys Res Oceans 119:5160–5180

Satake K (1986) Re-examination of the 1940 Shakotan-oki earthquake and the fault parameters of the earthquakes along the eastern margin of the Japan Sea. Phys Earth Planet Int 43:137–147

Satake K (1995) Linear and nonlinear computations of the 1992 Nicaragua earthquake tsunami. Pure Appl Geophys 144:455–470

Satake K, Abe K (1983) A fault model for the Niigata, Japan, earthquake of June 16, 1964. J Phys Earth 31:217–223

Tanioka Y, Satake K, Ruff L (1995) Total analysis of the 1993 Hokkaido Nansei-oki earthquake using seismic wave, tsunami, and geodetic data. Geophys Res Lett 22:9–12

Tsuji Y, Imai K, Sato M, Haga Y, Matsuoka Y, Imamura F (2014) Heights of the Tsunami of the Hoei earthquake of October 28th, 1707 on the coasts of Tanegashima Island and Nagasaki city. Rep Tsunami Eng 31:201–214 **(in Japanese)**

Wang F, Liu C, Zhang Z (2005) Earthquake tsunami record in Chinese ancient books. Earthq Res China 21:437–443 **(in Chinese)**

Wen YL, Zhao WZ, Li W, Xue Y, Yu HY (2014) Research on the potential tsunami hazard in east China coast under rare earthquake occurred in Nankai Trough, Japan. Acta Seismol Sin 36:651–661 **(in Chinese with English abstract)**